IEEE Access
Multidisciplinary | Rapid Review | Open Access Journal

Received December 11, 2018, accepted December 22, 2018, date of publication December 27, 2018, date of current version January 16, 2019.

Digital Object Identifier 10.1109/ACCESS.2018.2889874

Single RF-Chain Beam Training for MU-MIMO Energy Efficiency and Information-Centric IoT Millimeter Wave Communications

XIONGWEN ZHAO[1], (Senior Member, IEEE), ADAM MOHAMED AHMED ABDO[1,2], YU ZHANG[1], SUIYAN GENG[1], AND JIANHUA ZHANG[3], (Senior Member, IEEE)

[1]Electrical and Electronic Department, North China Electric Power University, Beijing 102206, China
[2]Electrical and Electronic Department, Faculty of Engineering Science, University of Nyala, Nyala 63312, Sudan
[3]State Key Laboratory of Networking and Switching Technology, Beijing University of Posts and Telecommunications, Beijing 100876, China

Corresponding author: Adam Mohamed Ahmed Abdo (adam_ma83@yahoo.com)

This work was supported in part by the National Nature Science Foundation of China (NSFC) under Grant 61771194, in part by the Key Program of the Beijing Municipal Natural Science Foundation under Grant 17L20052, and in part by the Beijing Municipal Science and Technology Commission under Grant Z181100003218007.

ABSTRACT In a multi-user multiple-input multiple-output (MU-MIMO) communication system, multiple RF (radio frequency) chains are generally connected corresponding to the antenna elements. However, the system complexity, hardware cost, and energy consumption are challenging while using many RF chains. In addition, an information-centric Internet of Things (IoT) will be significant to guarantee fast service demand for radio access in the fifth generation (5G) mmWave wireless systems. In this paper, a new beam training method based on a single RF chain is proposed to overcome these challenges by using the downlink–uplink and downlink–downlink beam training techniques to establish the elite users' subset group which can be trained in a single training time slot. Additionally, the users' subset mechanism is implemented by selecting an arbitrary function to guarantee the convergence. Moreover, the proposed techniques are compared with the conventional full search method regarding searching time, cost, and complexity. Different user subset functions are modeled, evaluated, and compared with the existing ones with respect to effective channel gain and average system capacity. The simulation results show that the proposed method can achieve a significant system performance, and the single RF chain is serviceable for a large number of users when connected with a maximum of 64 antenna elements at the BS. The proposed method can also be implemented in a massive MU-MIMO system by using multiple RF chains in which each RF chain is connected to a group of 64 antenna elements. This work is applicable in 5G mmWave communications, which require robust infrastructure to meet the future IoT service demand in 5G hot scenarios.

INDEX TERMS Millimeter wave (mmWave), radio frequency chain (RF-chain), beam training, downlink-uplink beam training, downlink-downlink beam training, elite users' subset, Internet of Things (IoT).

I. INTRODUCTION

Mllimeter wave (mm-Wave) communication is emerging to meet the increasing demand for high data rate transmission in dense populated areas, and it is a promising solution for radio access in future indoor and outdoor cellular systems [1]–[3]. Large multiplexing and array gains are offered by massive multiple-input multiple-output (MIMO) system, which makes it an attractive technology for the fifth generation (5G) mm-Wave communications [4]. On the contrary, the mm-Wave suffers from the huge path loss which makes it difficult in practical usage, particularly in dense urban areas [2], [5]. Therefore, large-scale directional antennas are packaged into small form factor to provide array gain and achieve reasonable link signal strength [6], [7]. Moreover, because of the short wavelength in mmWave band, it allows to use more antenna elements in a limited physical space [8].

MIMO systems can meet the demand of high data rate transmission and increase the spectral efficiency, conventional precoding and combiner have been widely used to allow MIMO systems to serve lots of users simultaneously. In [9]–[11], full digital precoding is applied, in which an

antenna element is assigned to a single radio-frequency (RF) chain.

However, to implement the precoding in a massive MIMO system with up to a hundred number of antenna elements will cause an unacceptable level of complexity, at the same time the large number of RF chains will cause high hardware cost, and energy consumption and dissipation, which will shorten the lifetime of the power sources [10]–[13]. As mentioned in [13], the RF chains almost consume up to 70% of the total transceiver power when one RF chain per antenna element is deployed. Moreover, using large number of RF chains will also cause a high complexity in signal generation and detection at both transceiver ends. Meanwhile, the base station (BS) cost in a massive MIMO system scales linearly with a vast number of antenna elements. Additionally, a non-negligible effect by using a large number of RF chains is the system noise which can be increased by using large amount of components. Therefore, it is challenging to realise the massive MIMO mmWave systems practically without finding some techniques to handle these challenges [13].

Antenna selection approach is often used to decrease the hardware complexity. However, it brings a significant effect on the system performance when MIMO system with full digital precoding is implemented [5], [14]. The number of selected antennas per user is different from user to user according to their channel state information (CSI). Meanwhile, it is challenging to design the precoding matrices (codebook) for all users simultaneously. While in [4] a RF antenna switch with constant phase shifter for a massive MIMO receiver was proposed, in which a low-complexity algorithm for the combination matrix in polynomial time was designed regarding the number of antenna elements. In particular, a low-complexity algorithm was applied to quasi-coherent combination which requires a small number of RF chains, rather than equivalent to the number of antenna elements. Hence, using less number of RF chains obviously can cause low power consumption in total. However, in [4] the number of switches is equal to the number of RF chains, which leads to the power consumption as well. In [6], a hybrid-digital/analog-precoding was fully employed with one-stage feedback technique aiming at the minimization of digital precoder interference, meanwhile it can reduce the feedback overhead effectively as well as the complexity. Moreover, the digital precoder and feedback overhead were used to mitigate the multiuser interference to design the first stage analog beamforming precisely. In [15] and [16], a method based on hybrid analog/digital precoding was proposed, in which the hybrid precoding was used in the BS, while the mobile station (MS) kept employing only analog combining. It was realized that the downlink MU-MIMO system achieved a significant performance with low complexity. Based on mean-squared error (MSE) criteria, a hybrid analog/digital precoding and combining schemes for a multiuser mmWave system were developed in [7] and [17], the schemes were divided into two sub-design parts. In the first part, the analog combiners were designed, while at the second part the hybrid precoders and combiners were jointly designed. It was found that the hybrid precoding design scheme can realize a significant spectral efficiency with lower complexity than the method proposed in [15]. A massive MU-MIMO hybrid precoding with finite dimensional channel model was studied in [18], where M angular bins were applied to the system to define the channel vector model. In [19], a low complexity estimation for a hybrid MU-MIMO mm-Wave system was introduced allowing to estimate the strongest angle of arrivals (AOAs) for the BS and MS contentiously. The method is practically sufficient with less cost using a small number of RF chains instead of a large number of antenna elements.

A MU-MIMO mmWave beam training system with a single RF chain at the BS was firstly introduced in [20], where the combination of the downlink-uplink sector sweep was carried out to find the effective channel gain for each user. Moreover, it was mentioned that the technique can achieve a higher performance than the exhaustive full search method. Meanwhile, by comparing with the conventional techniques, the single RF training method can achieve an acceptable system performance with low complexity and hardware cost.

The main objective of this paper is to reduce the energy consumption of the MU-MIMO system with low complexity and computation cost. A new beam training method based on a single RF chain is proposed instead of multiple RF chains. Interestingly, the state-of-art contains two types of beam training schemes, namely sequential downlink-uplink (SDU) and sequential downlink-downlink (SDD) beam training schemes. The proposed schemes are based on finding the subset group of users that can be trained in a single timeslot, which is called "elite user set $\left|\aleph^{\text{elite}}\right|$". Additionally, the line-of-sight (LOS) probability of each user regarding the BS is taken into account while setting up the elite user group. In this case, a specific path factor called β_{elite} is calculated based on the following parameters: the probability of LOS, coverage and steering angles, and number of paths. Simulation results show that the proposed beam training schemes are with low computation cost and less searching time compared with the conventional (full exhaustive search) method.

The rest of this paper is organized as follow. In section II, the system model including channel model, signal model, and the precoder and combiner are introduced. The detailed proposed single RF-chain beam training method is presented in section III. Section IV covers the simulation results and discussions, and the conclusions are drawn in section V.

The notations in this paper are as follow; boldface capital letters denote matrices and boldface lowercase letters denote column vectors, the superscript $(\cdot)^H$, $(\cdot)^T$ and $(\cdot)^*$ denote the conjugate-transpose (Hermitian), transpose and conjugate, respectively. $E\{\cdot\}$, $\mathbf{I}_N$, and $\mathbb{CN}$ are the expectation operator, square identity matrix of size $N \times N$, and Gaussian random complex numbers, respectively.

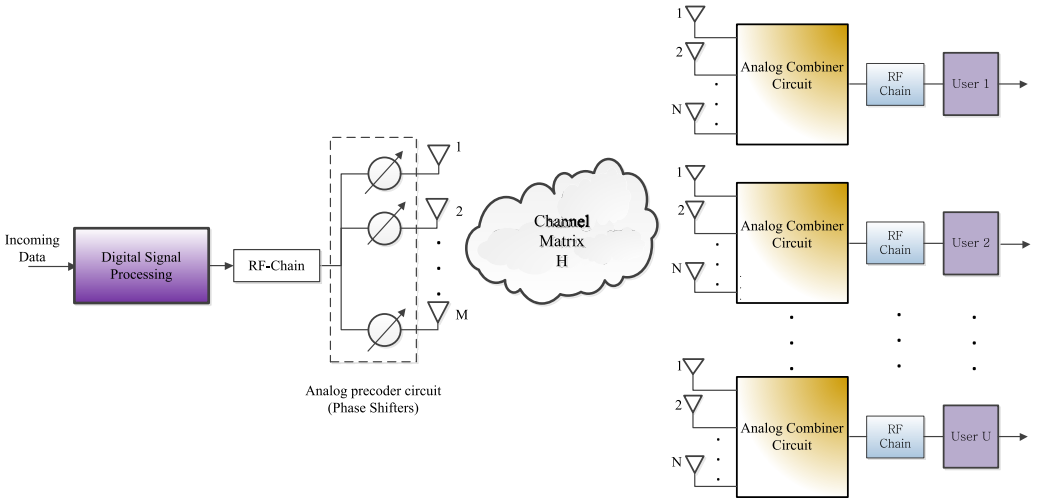

FIGURE 1. MU-MIMO IoT system model for mmWave communications.

II. SYSTEM MODEL

The general system model of this paper as shown in Fig. 1, a mmWave communication system with MU-MIMO transceiver is assumed, the model involves one BS to serve U number of users consecutively, by mapping all users in a subset groups according to their request. Meanwhile, the BS is represented by one RF chain connected with M linear array antenna elements to perform multi-user beamforming (precoding). Similarly, at the users' end, each user is represented by a single RF chain connected with N linear array antenna elements ($N \ll M$) to provide user's beam-forming (combiner) as well [21].

A. CHANNEL AND SIGNAL MODELS

In this subsection, the MU-MIMO system channel and signal models are described based on Fig. 1. The channel model is assumed to be Saleh-Valenzuela channel model, in which the multipath signals are taken into account [22]. In addition, due to small size of mmWave signal antenna element, and the capability of using the integration of a large number of directional antenna elements into a small form factor, most of the signal's energy can concentrate on the LOS path, while the small amount of energy will be distributed among the scattered signal paths. Consequently, the channel matrix $\mathbf{H} \in \mathbb{C}^{N\times M}$ for u^{th} user $\mathbf{H}_u(u = 1, 2, \ldots, U)$ can be constructed as follows:

$$\mathbf{H}_u = \sqrt{N * M} \sum_{l}^{L} \alpha_l * \mathbf{b}(\phi_l^r) * \mathbf{a}(\theta_l^t)^H \in \mathbb{C}^{N\times M} \quad (1)$$

where ϕ_l^r and θ_l^t are the azimuth angle of arrival (AoA) and azimuth angle of departure (AoD) for l^{th} path respectively. Besides, it is assumed that the AoA and AoD are uniformly distributed in the coverage beam angles (beam-width). Let us define $\phi_l^r \in \left[-\frac{\phi_{cov}}{2}, \frac{\phi_{cov}}{2}\right]$ and $\theta_l^t \in \left[-\frac{\theta_{cov}}{2}, \frac{\theta_{cov}}{2}\right]$, where ϕ_{cov} and θ_{cov} are in the range of $0 < [\phi_{cov}, \theta_{cov}] \leq \pi$. L and $\alpha_l \sim \mathbb{CN}(0, 1)$ are the number of multipath and the l^{th} path complex gain, respectively. Similarly, $\mathbf{a}(\theta_l^t)$ and $\mathbf{b}(\phi_l^r)$ are the transmitter and receiver array responses, respectively. Hereafter, these array responses are determined by the angles θ_l^t and ϕ_l^r as well as the geometry of the array antennas. In this work, the uniform linear array (ULA) antenna is assumed at both the transmitter and the receiver sides, hence the normalized ULA responses for the transceiver are as follow [2], [22]:

$$\mathbf{a}(\theta_l^t) = \frac{1}{\sqrt{M}}\left[1, e^{j\beta d\sin(\theta_l^t)}, \ldots, e^{j\beta d(M-1)\sin(\theta_l^t)}\right]^{\mathrm{T}} \in \mathbb{C}^{M\times 1} \quad (2)$$

$$\mathbf{b}(\phi_l^r) = \frac{1}{\sqrt{N}}\left[1, e^{j\beta d\sin(\phi_l^r)}, \ldots, e^{j\beta d(N-1)\sin(\phi_l^r)}\right]^{\mathrm{T}} \in \mathbb{C}^{N\times 1} \quad (3)$$

where $\beta = 2\pi/\lambda$, d is the spacing between antenna element which is equal to $\lambda/2$.

However, it is challenging to get a full channel state information (CSI) for the mmWave communications system, because of using limited number of RF chains when considering the cost issue. Therefore, the codebook based beamforming technique is an essential way to overcome this issue. Furthermore, the BS serves one user at each time slot through the RF beamforming weight vectors (code vectors or analog precoder). Consequently, the received signal symbol $s_u \in \mathbb{C}^{1\times 1}$ for u^{th} user can be expressed as:

$$s_u = \sqrt{\rho}\mathbf{w}_u^H \mathbf{H}_u \mathbf{f}_u x_u + \mathbf{w}_u^H \mathbf{n}_u \quad (4)$$

where ρ, x_u and $\mathbf{n}_u \in \mathbb{C}^{N\times 1}$ are the total transmitted power at the BS, the complex data signal for u^{th} user, and the additive complex white Gaussian noise vector, respectively. The transmitted data symbol x_u satisfies $\mathbb{E}\left\{|x_u|^2\right\} = 1$; where $\mathbb{E}\{.\}$ denotes the expectation operation, while $\mathbf{n}_u$ follows independent and identically distribution (i.i.d) as $\mathbf{n}_u \sim N_{\mathbb{C}}(0, \sigma_n^2\mathbf{I}_N)$. The vectors $\mathbf{f}_u \in \mathbb{C}^{M\times 1}$ and $\mathbf{w}_u \in \mathbb{C}^{N\times 1}$ are the complex analog precoder and combiner vectors,

respectively [23], [24]. Furthermore, the precoder $\mathbf{f}_u$ and the combiner $\mathbf{w}_u$ are normalized by the factors $1/\sqrt{M}$ and $1/\sqrt{N}$, respectively. Accordingly, the expression in (4) after normalization can be re-written as [14]:

$$s_u = \sqrt{\frac{\rho}{M * N}}\mathbf{w}_u^H \mathbf{H}_u \mathbf{f}_u x_u + \frac{1}{\sqrt{N}}\mathbf{w}_u^H \mathbf{n}_u \tag{5}$$

B. ANALOG PRECODER AND COMBINER

This subsection discusses the analog precoding and combiner for MU-MIMO system. Consequently, the structure of the transceiver codebooks are as follow. The transmitter analog precoder $\mathbf{F}$ and the receiver analog combiner $\mathbf{W}$ codebooks can be constructed using phase shifters without any changes in the amplitude. Hence, the codebooks function is to provide beamforming with different phase angles (different directions) with the same amplitude. Therefore, at both sides of the transceiver, a specific number of bits can be used for the phase angles quantization. Moreover, the selected number of quantization bits is proportional to the number of RF chains. However, the number of phase angles (phase shifters) depends on the number of antenna elements deployed at the transmitter and receiver sides. Explicitly, the sides of Fig.1 show that the phase shifters are connected to the RF-chain. Clearly, it is shown at the transmitter end, where a group of antenna elements are connected to the single RF-chain through the phase shifters. Similarly, at the receiver side in which the analog combiners are represented by blocks, and each block contains a number of antenna elements and phase shifters as well. Suppose we have Q_t and Q_r bits of discrete Fourier transform (DFT) codebook phase angles for the transmitter and the receiver, respectively. Then all possible number of RF beamforming vectors at the transmitter and the receiver are given by 2^{Q_t} and 2^{Q_r}, respectively, and the corresponding quantization phase angles are given as follow:

$$\theta_m^t \in \left\{ \frac{2\pi m}{2^{Q_t}} \middle| \quad m = 1, 2, \ldots, 2^{Q_t} \right. \tag{6}$$

and

$$\phi_n^r \in \left\{ \frac{2\pi n}{2^{Q_r}} \middle| \quad n = 1, 2, \ldots, 2^{Q_r} \right. \tag{7}$$

Consequently, assume $M_B = 2^{Q_t}$ and $N_B = 2^{Q_r}$ are respectively, the number of all possible generated beams at the transmitter and the receiver [22], [23]. In MU-MIMO it is possible to assume $Q_t > Q_r$, because the transmitter needs to handle many users' request instantly by constructing the precoding matrix, then from the previous assumptions certainly $M_B \gg N_B$. Subsequently, the codebook beam steering vectors for analog precoder can be mapped as $\mathbf{F} = \left[\mathbf{f}_1, \mathbf{f}_2, \ldots, \mathbf{f}_{M_B}\right]$. Likewise, the steering vectors can be re-written regarding the phase angles (AoD) as $\mathbf{F} = \left[\mathbf{a}(\theta_1^t), \mathbf{a}(\theta_2^t), \ldots, \mathbf{a}(\theta_{M_B}^t)\right]$. Similarly, the codebook beam steering for analog combiner (at user end) can be mapped as $\mathbf{W} = \left[\mathbf{w}_1, \mathbf{w}_2, \ldots, \mathbf{w}_{N_B}\right]$. Besides, the analog combiner vectors can be re-written concerning the phase angles (AoA) as $\mathbf{W} = \left[\mathbf{b}(\phi_1^r), \mathbf{b}(\phi_2^r), \ldots, \mathbf{b}(\phi_{N_B}^r)\right]$ [5], [23]. However, the system model in this paper considers implementation of a single RF chain at the BS and at each user ends. Therefore, these codebooks are constructed to be used sequentially. Accordingly, the BS serves one user at each single time slot by finding the optimum beam pair to meet the maximum channel gain, which is called "single RF chain beam training". Since each user is represented by one RF chain, then the total number of RF chains for the entire MU-MIMO system is equal to $U + 1$ as shown in Fig. 1. Therefore, the codebook is formed by the analog precoder and combiner pair $(\mathbf{w}_u, \mathbf{f}_u)$, will be used during the beam training at each timeslot to calculate the effective gain for u^{th} user.

III. THE PROPOSED BEAM TRAINING METHOD

In this section, the proposed beam training method based on a single RF-chain at the BS is discussed in detail. Certainly, by referring to Figs. 2 and 3, two types of beam training techniques, namely sequential downlink-uplink (SDU) and sequential downlink-downlink (SDD) are presented. In the downlink-uplink technique, the BS uses only one beam among an available number of beams at each training time. Moreover, all users have to use the active BS beams simultaneously to calculate their channel gain, by using the mapped precoder $\mathbf{w}_u$ from the BS codebook and user's combiner vector $\mathbf{f}_u$ as shown in Fig. 2. Accordingly, for all users, the resulting channel gains $\left|\mathbf{w}_u^H \mathbf{H}_u \mathbf{f}_u\right| : u = 1, 2, \ldots, U$ are reported to the BS. Finally, the BS assigns the precoder vector $\mathbf{w}_u$ to the user who has reported the maximum channel gain. Meanwhile, the user will use this precoder with the analog combiner $\mathbf{f}_u$ to achieve the maximum transmission efficiency. Since the BS needs M_B timeslots so that to allow all users to find their best precoder/combiner codebook vectors, and each user needs N_B time slots to train all available codebook beams. Meanwhile, for the whole MU-MIMO system, the required number of timeslots is given by $t_{\text{slots}}^* = M_B + U * N_B$. However, the equivalent number of timeslots when using a full exhaustive technique for the same system is given by $t_{\text{slots}}^{\wedge} = M_B * N_B$. In downlink-downlink beam training technique as shown in Fig. 3, the BS uses all available beams as quasi omni-sector (concurrently). Meanwhile, during the coherence time interval T, the BS sets all codebook beams in active mode. Since each user has a possible N_B beams and $N_B \ll M_B$, the BS allows all users to find their optimum beam pair sequentially within the training time. Thus, the required number of timeslots is given by $\tilde{t}_{\text{slots}} = N_B + M_B$. Let us define $B_{\max}$ to be the maximum number of beams in single RF-chain in the system. In general, the maximum number of beams per single RF-chain in the MU-MIMO system can be determined by $B_{\max} = \max(M_B, N_B)$. However, in this study the number of beams at user side is much smaller than that in the BS, thus $B_{\max}$ becomes M_B.

For the sake of evaluation, the computation cost in terms of the required number of timeslots at the BS to serve all users is conducted. Moreover, the two techniques are compared

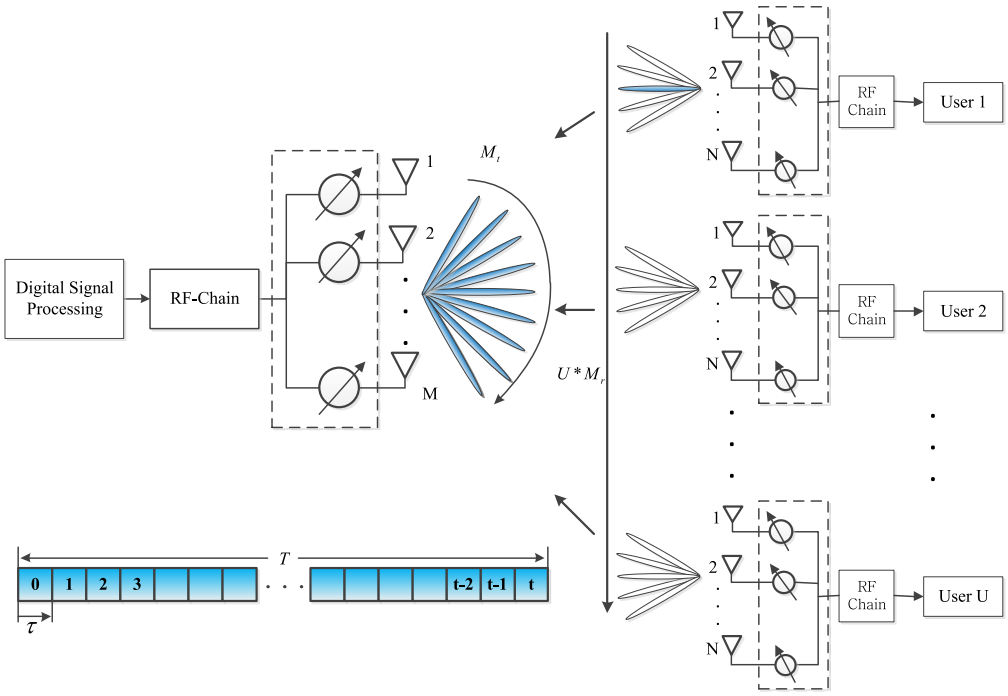

FIGURE 2. Schematic diagram for improvement of the sequential downlink-uplink beam training (SDU).

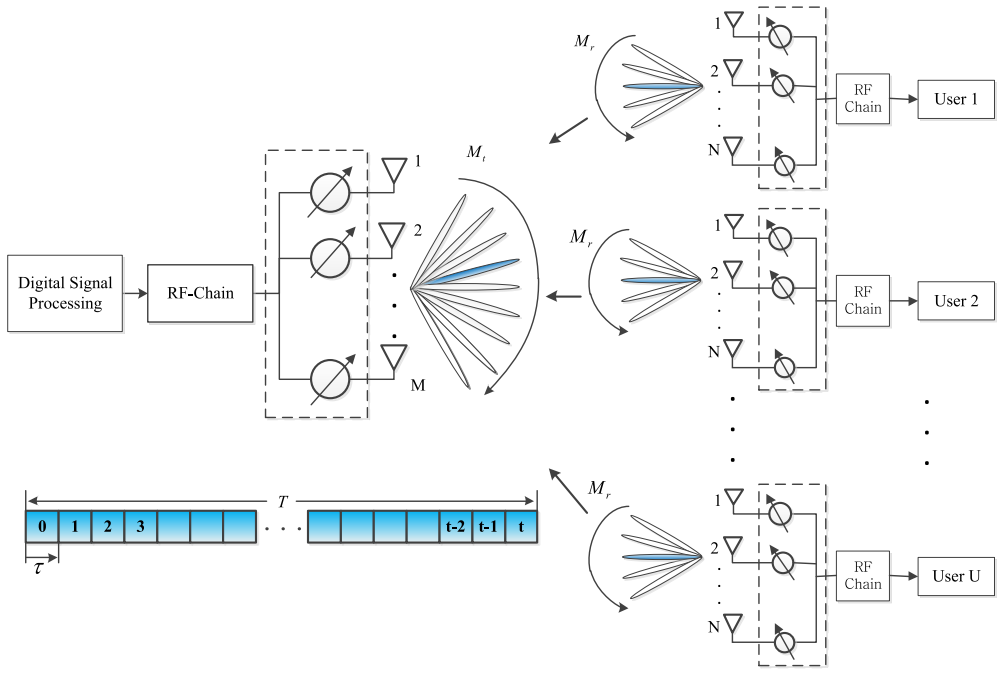

FIGURE 3. Schematic diagram for improvement of the sequential downlink-downlink beam training (SDD).

with the conventional full exhaustive technique as shown in Fig. 4. It is observed that the required number of timeslots is directly relational with the maximum number of beams $B_{\max}$. In addition, the number users U has a significant impact on the required number of timeslots which can be clearly realized in Fig. 3. Moreover, Fig. 4 shows the required number of timeslots in the SDD technique increases linearly with the slope of U. However, the required number of timeslots in the SDU beam training technique is much smaller than that in SDD, of course, this is due to independent from U. Explicitly, the required time slot in the exhaustive conventional method is dramatically increased with increasing $B_{\max}$.

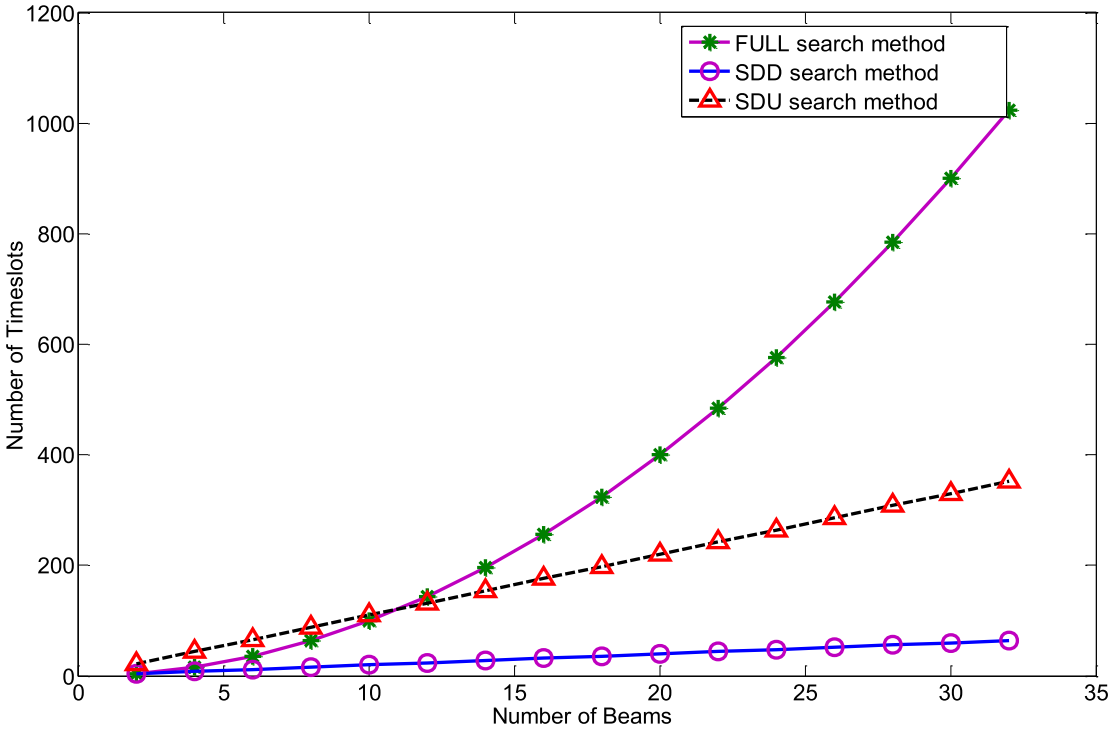

FIGURE 4. Beam training cost of the proposed methods regarding the conventional exhaustive full search method.

Hence, the proposed two techniques are with low beam training cost compared to the conventional full search method.

A. FINDING THE OPTIMUM CHANNEL GAIN

In this subsection, the channel gain is calculated based on optimal beam searching techniques. In this case, the optimal beam pair that maximizes the signal strength of u^{th} user is subjected to channel gain magnitude. Furthermore, the channel gain is determined by; the channel matrix $\mathbf{H}_u$, predefined codebooks matrices $\mathbf{F} \in \mathbb{C}^{M\times M_B}$ and $\mathbf{W} \in \mathbb{C}^{N\times N_B}$ at the BS and users' end, respectively. For u^{th} user the effective channel gain can be defined as follows:

$$\eta_u(\mathbf{f}_{u,m}, \mathbf{w}_{u,n}) = \left|\mathbf{w}_{u,n}^H \mathbf{H}_u \mathbf{f}_{u,m}\right|^2 \tag{8}$$

where m and n are the codebooks indexes which are described in (6) and (7), respectively.

Interestingly, the optimum beam pair index for u^{th} user can be determined as:

$$\left\{\hat{m}_u, \hat{n}_u\right\} = \arg\max_{\{m,n\}} \eta_u(\mathbf{f}_{u,m}, \mathbf{w}_{u,n}) \tag{9}$$

Subsequently, the BS selects the entry of the codebook with the highest gain by $\hat{u} = \max \eta_u(\mathbf{f}_{u,\hat{m}}, \mathbf{w}_{u,\hat{n}})$, $u \in \aleph$, where $\aleph$ is the total user subset, and it satisfies $|\aleph| = U$.

The similar training timeslot duration called alignment time period τ is implemented in [1], and it can be used to calculate the achievable sum rate. However, in this work the effective user data rate can be calculated by substituting τ with the number required timeslots t_{slots}.

Accordingly, the achievable sum rate regarding SINR in [1] can be adopted as follows:

$$C = \left(1 - \frac{t_{\text{slots}}}{T}\right) \log_2 (1 + \text{SINR}) \tag{10}$$

where T denotes the training period (coherence interval).

For clarity the coherence time T can be expressed in terms of number of timeslots, assume we have time block with period T, and assume this period is divided into many timeslots, and each slot with a duration of τ_{d}. Accordingly, it is possible to have different length of T by increasing the number of slots and fixing the slot duration τ_{d}. Hence the number of timeslots is increases by increasing the length of coherence time T. From this perspective, we can express T by the number of timeslots, for more explanation refer to time diagram of Figs. 2 and 3. Accordingly, the system sum rate capacity in (10) can be recalculated by including the effective users' channel gain which is presented in (8). In addition and by re-writing the SINR in terms of the total transmission power P_{BS} and the average noise power $\sigma^2 = \mathbb{E}\left|\mathbf{n}_u^H \mathbf{n}_u\right|$, then the achievable sum-rate capacity can be expressed as follows:

$$C = \left(1 - \frac{t_{\text{slots}}}{T}\right) * \text{E}\left[\log_2\left(1 + \frac{P_{\text{BS}}}{\sigma^2}\eta_{\hat{u}}\right)\right] \tag{11}$$

Obviously, the average achievable sum rate is inversely proportional with t_{slots}. Also, when the coherence time T is large enough and t_{slots} is very small ($1 \gg \frac{t_{\text{slots}}}{T}$), the achievable sum rate will get the maximum value. Particularly, in mmWave band because the frequency band is much higher in (GHz),

compared with radio frequency and microwave bands in which the slot duration is much longer than in mmWave band. Besides, when the number of users U goes to infinity ($U \to \infty$), the expression in (11) can be approximated as:

$$C = \mathrm{E}\left[\log_2\left(1 + \frac{P_{\mathrm{BS}}}{\sigma^2}\eta_{\hat{u}}\right)\right] \cong \log_2\left(1 + \frac{M * N * P_{\mathrm{BS}}}{\sigma^2}\log_{10} U\right) \quad (12)$$

Furthermore, the BS selects a set of users in a group to perform the training during each training period, this group is called "*elite*" user subset, and it is denoted by $\left|\aleph^{\mathrm{elite}}\right|$. For the sake of the simplicity, let us define $G = \frac{M*N*P_{\mathrm{BS}}}{\sigma^2} = M * N * \rho$, where $\rho = \frac{P_{BS}}{\sigma^2}$. Thus, the average upper bound capacity can be defined as the overall system capacity which can be achieved, when the BS has an ability to serve all users simultaneously according to their service request. In this case, the maximum average system capacity is denoted by upper bound system capacity, and it can be given as:

$$C_{\mathrm{upper}} \leq \log_2\left(1 + G * \log_{10} U\right) \quad (13)$$

By recalling the elite user set grouped by the BS, the average sum-rate capacity can be calculated by the selected elite group $\left|\aleph^{\mathrm{elite}}\right|$. Meanwhile, the new average achievable sum-rate is considered as a lower bound capacity which varies with the users' subset size, then the form in (13) can be re-written as:

$$C_{\mathrm{lower}} \geq \log_2\left(1 + G * \log\left|\aleph^{\mathrm{elite}}\right|\right) \quad (14)$$

B. DETERMINING THE ELITE USER SUBSET $\left|\aleph^{elite}\right|$

This subsection introduces the design of elite function, which subjected to a fixed conditions that guarantee the convergence of the training methods [20], [25]. Hence, based on the steering array vectors as well as the precoder and combiner vectors phase angles, we can have the follows formula:

$$\aleph^{\mathrm{elite}} = \begin{cases} u \in U : \left|\sin\left(\theta_l^t\right) - \sin\left(\theta_m^t\right)\right| \leq \dfrac{1}{\varepsilon(U)} \\ \text{and} \\ \left|\sin\left(\phi_l^r\right) - \sin\left(\phi_n^r\right)\right| \leq \dfrac{1}{\varepsilon(U)} \\ \forall : l \in L, \quad m \in M_{RF},\ n \in N_{RF} \end{cases} \quad (15)$$

where $\varepsilon(U)$ is an arbitrary function which is selected to satisfy certain conditions as expressed in (16).

In [20], the arbitrary function $\varepsilon(U)$ was taken as $\varepsilon\,(U) = \log_{10}(U)$. It is realized that this function has a good tendency when U goes to infinity, and also to get a better function convergent. However, the function is subjected to the conditions in (16). In fact it is challenging to get an arbitrary function $\varepsilon(U)$ that can satisfy all the conditions in (16) at the same time.

Nevertheless, in a practical MU-MIMO mmWave communication system, the BS serves a finite number of users U. Therefore, in this study a new arbitrary functions are proposed, in which the conditions in (16) are not essential to be satisfied, but all the functions are validated for a good convergence. Accordingly, the function $\varepsilon\,(U)$ is assumed to be a logarithmic function as demonstrated in (17).

$$\begin{cases} \lim\limits_{U\to\infty} \frac{1}{\varepsilon(U)} \to 0 & (a) \\ \lim\limits_{U\to\infty} \frac{U}{\varepsilon(U)^{2L}} \to \infty & (b) \\ \lim\limits_{U\to\infty} \frac{\sqrt{\log U}}{\varepsilon(U)^2} \to 0 & (c) \\ \lim\limits_{U\to\infty} \frac{U\frac{d\varepsilon(U)}{dU}}{\varepsilon(U)} \to 0 & (d) \end{cases} \quad (16)$$

Likewise, it is an essential to consider the tendency of any new model when proposed to be implemented on a given system. In this regard, mostly the logarithmic function is much efficient to obtain the convergence of the functions according to the required conditions. Hence, the expressions in (17) are conducted to validate the analytical results regarding the increasing number of user U, as well as to find a close form solution of elite user's subset.

$$\varepsilon(U) \in \begin{cases} \log\left(\mathrm{f}_1(U)\right) = \log\left(\sqrt{U}\Big/\left(\sqrt{U+1} - \sqrt{U}\right)\right) \\ \log\left(\mathrm{f}_2(U)\right) = \log\left(1\Big/\left(\sqrt{U+1} - \sqrt{U}\right)\right) \\ \log\left(\mathrm{f}_3(U)\right) = \log\left(\sqrt[3]{U}\right) \end{cases} \quad (17)$$

However, there is one more condition that is restricted to the selected arbitrary functions, namely a uniqueness of the limit. The purpose of the theorem is to confirm that any of these functions have only one solution when the limit of the function is defined.

Definition of the uniqueness of limit; *Let us suppose the Value:*

Z is the limit of the sequence a_n, and for a given small value $\varepsilon > 0$, $a_n \underset{\varepsilon}{\approx} Z$ for $n \gg 1$. If such condition is satisfied, then Z is existent, and we can say that $\{a_n\}$ is convergent, otherwise, it is divergent.

Accordingly, the convergence conditions can be written as $\lim\limits_{n\to\infty}\{a_n\} = Z$, $a_n \to Z$ and $n \to \infty$. Additionally, the limit theorem can be expressed as $\lim a_n = Z$ or $a_n \to Z$. Thus, there is only one limit for the sequence a_n, in other words, if $a_n \to l$ and $a_n \to m$ then $l = m$. In consequence, this theorem can be concluded as follows:

Suppose a_n is a sequence and $l, m \in \mathbb{R}$ are the limits of a_n, then $l = m$. ***See the Proof in Appendix***.

Finally, based on these functions, when the number of user ($U \to \infty$) goes to infinity, we can get the approximation $\varepsilon\,(U)^{2L} \approx U\beta_{elite}/\left|\aleph^{\mathrm{elite}}\right|$, where β_{elite} is alignment factor, which is used to determine the possibility of available LOS alignment between the BS and end users during the training period. So, the alignment factor can be modeled as follows:

$$\beta_{elite} = \mathrm{Pr}_{LOS}^{BS\leftrightarrow U} \sum_{l}^{L}\left(\frac{2}{\theta_{cover}\sin\theta_l^r}\right)^L \sum_{l}^{L}\left(\frac{2}{\phi_{cover}\sin\phi_l^t}\right)^L \quad (18)$$

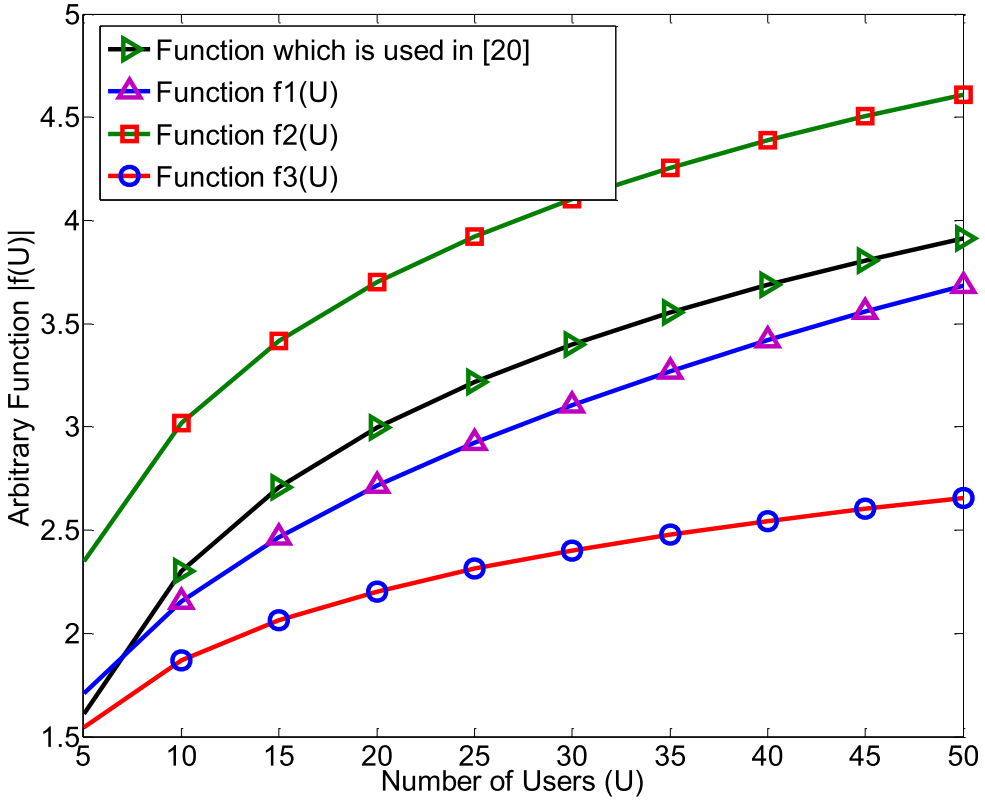

FIGURE 5. Absolute value of the selected arbitrary functions $\varepsilon(U)$ regarding the number of users U.

where $\Pr_{LOS}^{BS\leftrightarrow U}$ is the LOS probability, and it is described as the probability of the LOS path, in which no blockage existences between the BS and end user. In addition, the probability of LOS depends on the distance between BS and each user (distance $d^{BS\leftrightarrow U}$), as well as the user densities in a service area, i.e. rural, suburban, and urban areas, while the urban area is assumed in this work, and the $\Pr_{LOS}^{BS\leftrightarrow U}$ of LOS can be modeled as follows [27]:

$$\Pr_{LOS}^{BS\leftrightarrow U} \simeq \min\left(\frac{A}{d^{BS\leftrightarrow U}}, 1\right)\left(1 - e^{-\frac{d^{BS\leftrightarrow U}}{B}}\right) + e^{-\frac{d^{BS\leftrightarrow U}}{B}} \tag{19}$$

where $A = 18$ meters and $B = 63$ meters for urban density areas, as demonstrated in [24] and [26].

Interestingly, from the arbitrary function models, the magnitude of the functions are plotted as dB to recognize the convergence of each function. Accordingly, Fig. 5 is provided to show the magnitude tendency of selected functions with respect to the number of users. It is realized that all the functions in (17) are converged.

Subsequently, by recalling the alignment factor in (18), the user subset $\left|\aleph^{\text{elite}}\right|$ can be determined as:

$$\left|\aleph^{\text{elite}}\right| \in \begin{cases} \beta_{elite} U / \log\left(\mathrm{f}_1\left(U\right)^{2L}\right) \\ \beta_{elite} U / \log\left(\mathrm{f}_2\left(U\right)^{2L}\right) \\ \beta_{elite} U / \log\left(\mathrm{f}_3\left(U\right)^{2L}\right) \end{cases} \tag{20}$$

Hence, for the sake of validation, based on (20) the elite user subset result regarding the number of users is obtained, as shown in Fig. 6 it is observed that the user subset $\left|\aleph^{\text{elite}}\right|$ is affected by the three factors; the number of users, the arbitrary function model, and the alignment factor.

In addition, the user subset model $\left|\aleph^{\text{elite}}\right|$ can be used to evaluate and prove the system capacity, regarding the mean gap-loss capacity between the upper-bounded and lower-bounded capacities. Remarkably, from (13) and (14), the mean gap-loss which is the difference between upper and lower capacities can be calculated as [14]

$$\Delta R^{\text{Upp-Low}} = C_{\text{Upp}} - C_{\text{Low}} \tag{21}$$

By substituting (13) and (14) in (21), we will get

$$\Delta R^{\text{Upp-Low}} = \log_2\left(1 + G * \log U\right) - \log_2\left(1 + G * \log\left|\aleph^{\text{elite}}\right|\right) \tag{22}$$

Furthermore, by using logarithmic rules, the quantity in (22) can be re-written as

$$\Delta R^{\text{Upp-Low}} = \log_2\left(\frac{\left(1 + G * \log U\right)}{\left(1 + G * \log\left|\aleph^{\text{elite}}\right|\right)}\right) \tag{23}$$

On the other hand, to evaluate the beam training techniques in Figs. 2 and 3, the ratio between the techniques regarding the full exhaustive search method are provided. Moreover, as discussed at the beginning of this section that

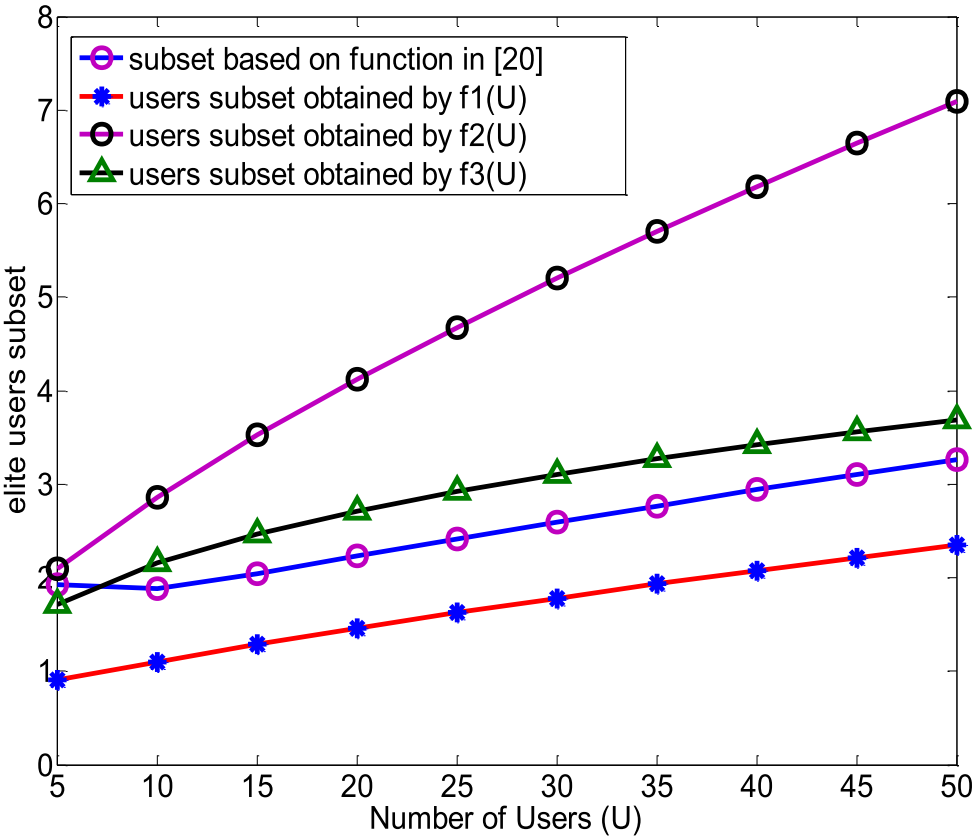

FIGURE 6. The user subset or elite group ($|\aleph^{\text{elite}}|$) regarding the number of users.

the required number of timeslots for the downlink-downlink and downlink-uplink techniques are $\tilde{t}_{\text{slots}}$ and t^*_{slots}, respectively. Therefore, by using (11) and substituting t_{slots} with $\tilde{t}_{\text{slots}}$ and t^*_{slots} as well as by re-writing once again the required number of timeslots $\tilde{t}_{\text{slots}}$ and t^*_{slots} as a function of M_B, N_B and U. Then we can get the system capacity for each technique and also to show their impacts to the average system capacity. Finally, the average system capacities for the full exhaustive search C^{Full}, downlink-uplink $C^{\text{DL-UL}}$ and downlink-downlink $C^{\text{DL-DL}}$ techniques can be expressed as in eqns. (24), (25) and (26), respectively.

$$\begin{aligned} C^{\text{Full}} &= \left(1-\frac{\hat{t}_{\text{slots}}}{T}\right) * \left[\log_2\left(1+\frac{P_{\text{BS}}}{\sigma^2}\eta_{\hat{u}}\right)\right] \\ &= \left(1-\frac{M_B * N_B}{T}\right) * \left[\log_2\left(1+\frac{P_{\text{BS}}}{\sigma^2}\eta_{\hat{u}}\right)\right] \quad (24) \\ C^{\text{DL-UL}} &= \left(1-\frac{t^*_{\text{slots}}}{T}\right)\left[\log_2\left(1+\frac{P_{\text{BS}}}{\sigma^2}\eta_{\hat{u}}\right)\right] \\ &= \left(1-\frac{(M_B+UN_B)}{T}\right)\left[\log_2\left(1+\frac{P_{\text{BS}}}{\sigma^2}\eta_{\hat{u}}\right)\right] \quad (25) \\ C^{\text{DL-DL}} &= \left(1-\frac{\tilde{t}_{\text{slots}}}{T}\right)\left[\log_2\left(1+\frac{P_{\text{BS}}}{\sigma^2}\eta_{\hat{u}}\right)\right] \\ &= \left(1-\frac{(M_B+N_B)}{T}\right)\left[\log_2\left(1+\frac{P_{\text{BS}}}{\sigma^2}\eta_{\hat{u}}\right)\right] \quad (26) \end{aligned}$$

Besides, the capacity ratio (gain) is a new metric factor can be obtained for the DL-UL and DL-DL techniques regarding the full exhaustive search method. Meanwhile, the ratio of DL-UL model to full exhaustive search technique, and the ratio of DL-DL model to full exhaustive search method are expressed as in (27) and (28), respectively.

$$\begin{aligned} &\Upsilon^{DL-UL} \\ &= \frac{C^{\text{DL-UL}}}{C^{\text{Full}}} = \left(1-\frac{(M_B+UN_B)}{T}\right) \Big/ \left(1-\frac{M_B * N_B}{T}\right) \quad (27) \\ &\Upsilon^{DL-DL} \\ &= \frac{C^{\text{DL-DL}}}{C^{\text{Full}}} = \left(1-\frac{(M_B+N_B)}{T}\right) \Big/ \left(1-\frac{M_B * N_B}{T}\right) \quad (28) \end{aligned}$$

Explicitly, it is observed from (27) and (28) that the capacity gains depend on both of the coherence time and the number of timeslots.

IV. SIMULATION RESULTS AND DISCUSSION

Simulation results are carried out in this section to validate our proposed techniques by comparison with conventional ones, in the simulations it's assumed that the mmWave carrier frequency is 26 GHz. Moreover, the system model consists of a BS equipped with a single RF chain which is connected with $M = 64$ antenna elements. Although, the number of antenna elements is supposed to be more than 64 elements especially

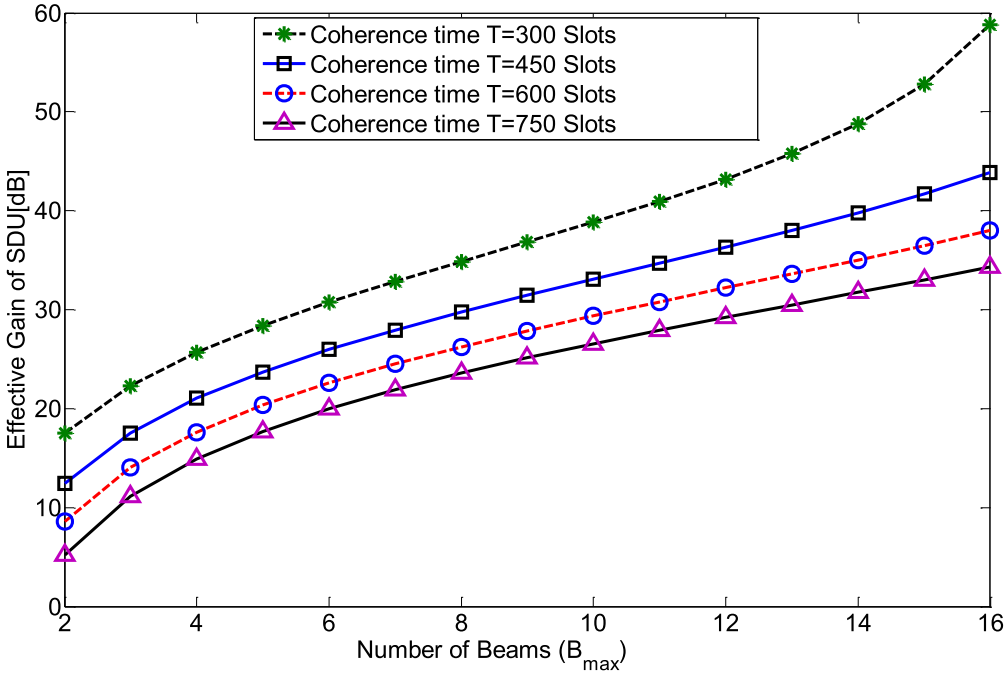

FIGURE 7. Effective gain of the SDU beam training method as a function of number of beams regarding the coherence time.

in a massive mmWave communication system. However, the degrees of freedom (DOF) do not allows a single RF chain to handle much more antenna elements. Furthermore, it's assumed that the maximum number of users is 50, and all users are supposed to have a normal distribution in an urban environment with a radius of 100 meters. Besides, each user is equipped with not more than four antenna elements $N \leq 4$. Finally, our proposed beam training techniques are evaluated in terms of the effective channel gain regarding the maximum number of training beams at the BS ($B_{\max}$) with different values of coherence time T. Likewise, based on the designed elite user subset functions, the average system and the gap loss (upper-lower) capacities are obtained.

However, this paragraph is provided to evaluate the performance of SDU and SDD techniques regarding the system capacity gain. Thus, the results in Fig. 7 and Fig. 8 are obtained based on the models in (27) and (28), respectively. For the sake of simplicity, the number beams at the BS is taken to be in the range of $2 \sim 16$ with different values of coherent time T. Fig. 7 shows the capacity gain of SDU technique, it is realized that the number of beams $B_{\max}$ and the coherence time have a significant impact on the system capacity gain. Obviously, e.g. when $T = 300$ timeslots, the corresponding capacity gains for $B_{\max} = 2$ and $B_{\max} = 16$ are approximately 20dB and 60dB, respectively.

Similarly, Fig. 8 demonstrates the capacity gain of SDD technique regarding the number of beams and different values of T. It is observed that the higher system capacity gain can be achieved with a smaller values of T and vice versa. On the other hand, it is realized that the capacity gain is directly proportional to the number of beams, in which the number of beams has a positive impact on system gain. Meanwhile, It is interesting to note that the average capacity gain of the SDU is much better than the SDD gain, e.g. the SDU and SDD achieve maximum capacity gains of about 60 dB and 17 dB, respectively, with 16 beams and $T = 300$ timeslots. This is due to the impact of the number of users U on the SDU capacity gain, as mentioned by the model in (27).

Fig. 9 shows the average system capacity (sum-rate capacity in bps/Hz) for upper and lower bound capacities as modeled in (13) and (14), respectively. In this case, different user subset elite functions are used to get the lower bound capacities. Interestingly, it is seen from Fig. 9 that when using the elite user subset functions, the upper bound capacity is in the range of about 13 -14 bps/Hz. Hence, by comparing the lower bound sum-rate capacity achieved by different elite user subset functions, it is observed that $\mathrm{f}_2(U)$ can achieve much better performance than the other functions, almost 1 bps/Hz less than the upper bound, while $\mathrm{f}_1(U)$ has the worst performance. Moreover, the performance of the elite user subset function in [20] is between $\mathrm{f}_3(U)$ and $\mathrm{f}_2(U)$.

Fig. 10 shows the gap-loss capacity to measure the capacities difference between the upper and lower bounds regarding the elite user subset functions. It is seen that, $\mathrm{f}_2(U)$ achieves a minimum gap-loss capacity of 1.2bps/Hz. While the gap-loss capacity of $\mathrm{f}_1(U)$ reaches the maximum of 6 bps/Hz, when the number of users is 5 as shown in the result. However, the gap-loss capacities for $\mathrm{f}_3(U)$ and the function in [20] are in the range of 1.2-1.8 bps/Hz. It's seen from Figs. 9 and 10, the selection of elite user subset functions are important

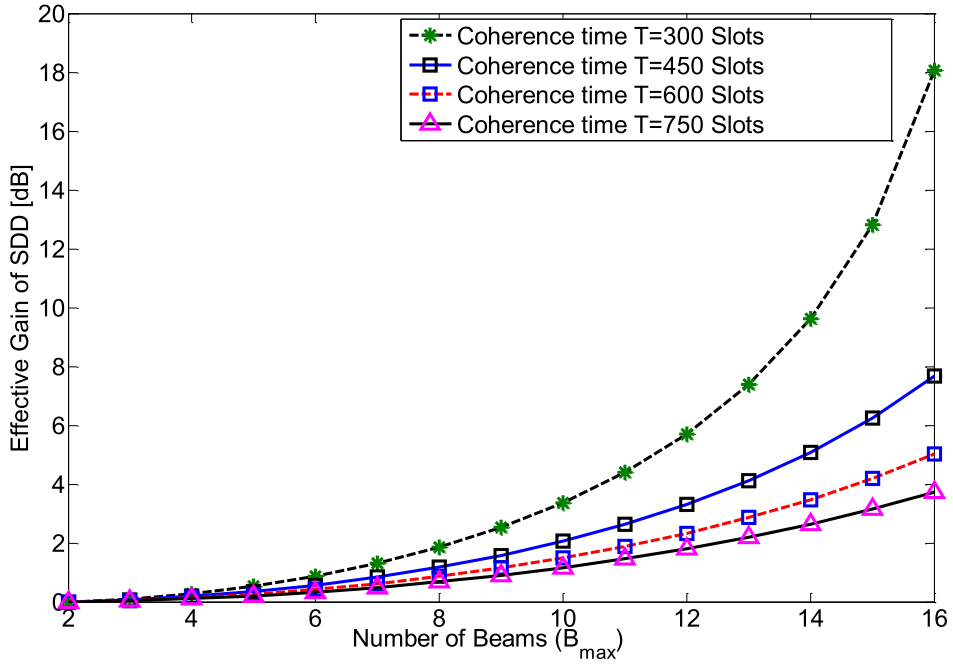

FIGURE 8. Effective gain of the SDD beam training method as a function of number of beams regarding the coherence time.

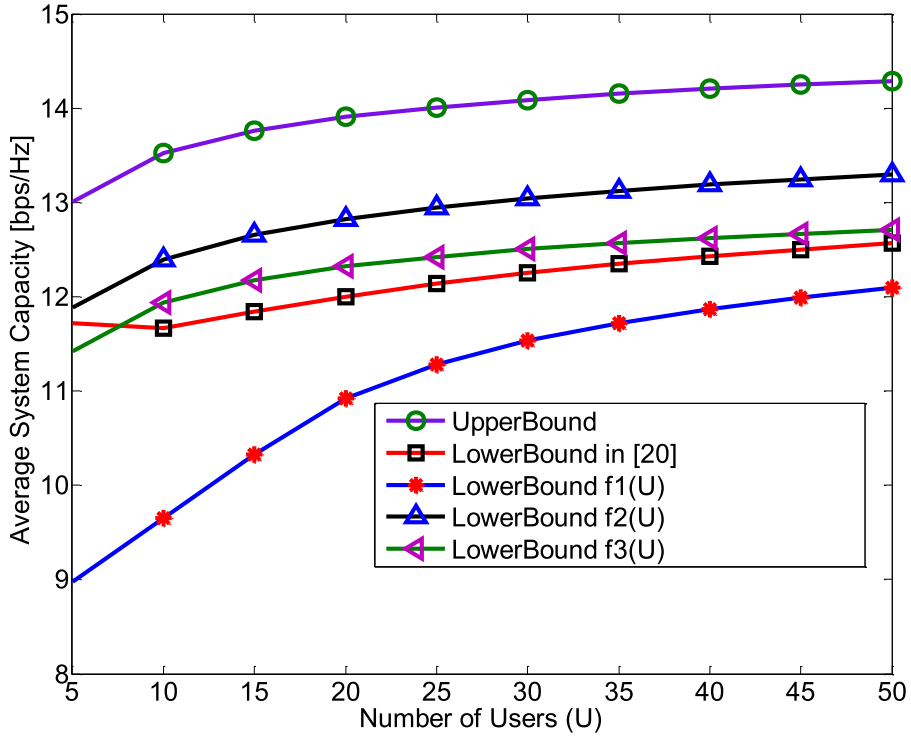

FIGURE 9. Upper and lower bounds of the average system capacities with respect to the number of users and user subset functions.

in calculating the average system and gap-loss capacities. Moreover, by comparison of the proposed techniques with the conventional one, the function $f_1(U)$ achieves lower performance than the conventional method. However, $f_2(U)$ and $f_3(U)$ achieve a higher performance relatively and $f_2(U)$ is the best. Fig. 11 shows the system achievable sum-rate

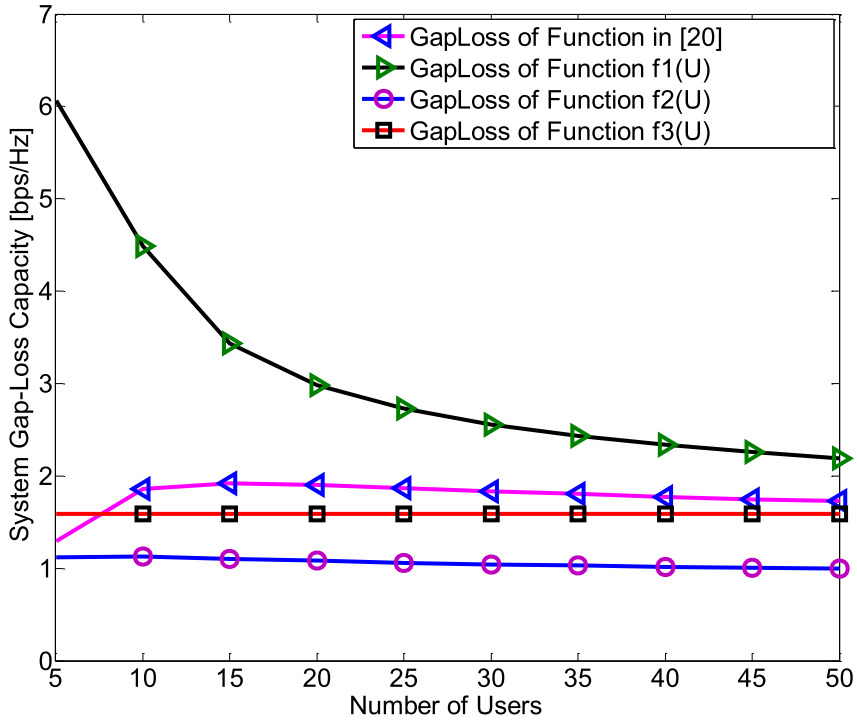

FIGURE 10. Capacity gap-Loss between upper- and lower-bound capacities with respect to the number of users and user subset functions.

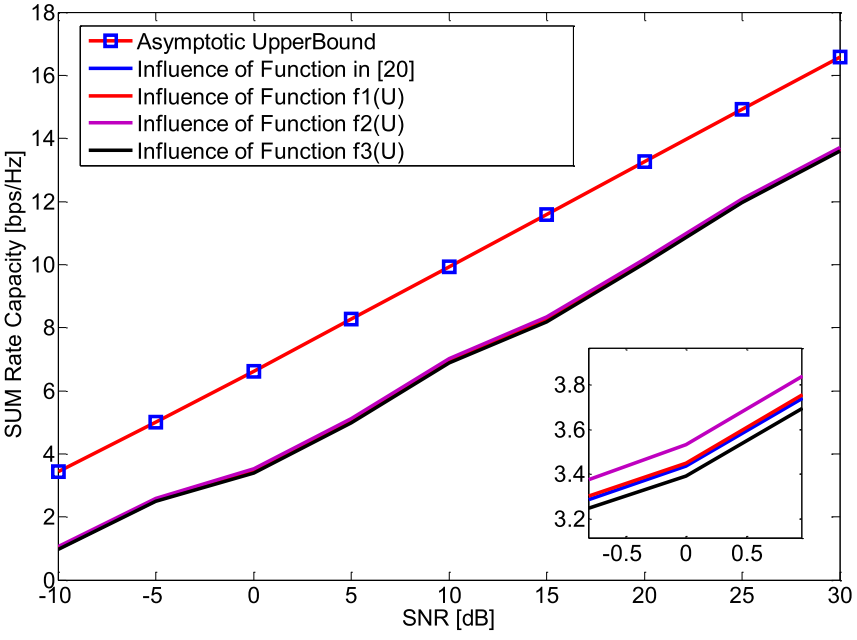

FIGURE 11. Average achievable sum rate capacity with respect to the signal to noise ratio ρ.

capacity regarding the SNR, where SNR (ρ) is assumed to be in the range of $[-10, 30]$ dB, it is realized that the upper-bound and lower bound capacities are dependent on the SNR. Similarly, it is observed that all the elite user subset functions achieve the similar performance except the upper-bound capacity, in which the achieved system capacity is approximately 2 bps/Hz higher than the lower-bound capacities. Meanwhile, the SNR impact is asymptotically equal for all users' subset functions. However, in Fig.11 e.g. by taking the SNRs in the range of $[-0.5, 0.5]$ dB, the corresponding

achieved capacities are in the range of 3.2 $\sim$ 3.8bps/Hz. Therefore, we can conclude that there is insignificant impact of SNR on the user subset functions. So, certainly not a significant difference in the average system capacity regarding the different functions can be recognized.

V. CONCLUSION

In this work, we proposed a new beam training methods (SDU and SDD) to be implemented for a single RF chain targeting to increase the energy efficiency and data transmission for 5G MU-MIMO IoT mmWave Communications. The elite user subset functions are selected and validated during training period. Besides, the proposed methods are compared with the conventional full search scheme regarding the effective channel gain and average system capacity. It's found that our proposed methods can work much better with lower searching time, computation complexity as well as hardware cost. Meanwhile, the simulation results show that our proposed methods can achieve efficient system performance using a single RF chain to be connected with maximum 64 antenna elements to serve a large number of users, and the elite function $f_2(U)$ indicates to be much better than the function proposed in [20]. As future work, our proposed methods are expected to be implemented in massive MU-MIMO mmWave system with multiple RF chains, in which each RF chain can be connected to a group of 64 antenna elements.

APPENDIX
PROOF OF THEOREM

The proof is started with an assumption of a_n which converges to both $l\&m$. In the following, we will prove that l should be equal to m. Let's first assume $l \neq m$

$$\forall \varepsilon > 0, \quad \exists N \in \mathbb{N}, \ \forall n \in \mathbb{N} \, (n \geq N \, |a_n - l| < \varepsilon) \tag{29}$$

$$\forall \varepsilon > 0, \quad \exists N \in \mathbb{N}, \ \forall n \in \mathbb{N} \, (n \geq N \, |a_n - m| < \varepsilon) \tag{30}$$

Note that when using the two statements of (29) and (30), we need a positive values of ε. Since $l \neq m$, the sequence a_n settles down about l or m, and they are away from each other. Hence, we can try to take the values of ε as in (31)

$$\varepsilon \in \left\{ \frac{1}{2} |l - m| \, , \frac{1}{3} |l - m| \, , \frac{1}{4} |l - m| \, , \ldots \right. \tag{31}$$

Let's select $\varepsilon = \frac{1}{2} |l - m|$, if a_n converges to l, suppose $N \in \mathbb{N}$ and $\forall n \in \mathbb{N} \frac{n!}{r!(n-r)!} (n \geq N_1 \Rightarrow |a_n - l| < \varepsilon)$. If a_n converges to m, suppose $N_1 \in \mathbb{N}$ and $\forall n \in \mathbb{N} (n \geq N_2 \Rightarrow |a_n - m| < \varepsilon)$. We can take the value of n as the maximum one between N_1 and N_2. Hence, $n = \max(N_1, N_2)$ then $|a_n - l| < \varepsilon$, $|a_n - m| < \varepsilon$, and $|l - m| \leq |a_n - l| + |a_n - m| < 2\varepsilon$ (triangle inequality), it means that $|l - m| < 2\varepsilon = 2 * \frac{1}{2} |l - m| = |l - m|$, which is impossible. Therefore, the sequence a_n should have only one limit, namely $l = m$.

REFERENCES

[1] A. Alkhateeb, O. El Ayach, G. Leus, and R. W. Heath, Jr., "Channel estimation and hybrid precoding for millimeter wave cellular systems," *IEEE J. Sel. Topics Signal Process.*, vol. 8, no. 5, pp. 831–846, Oct. 2014.

[2] X. Zhao, A. M. A. Abdo, C. Xu, S. Geng, J. Zhang, and I. Memon, "Dimension reduction of channel correlation matrix using CUR-decomposition technique for 3-D massive antenna system," *IEEE Access*, vol. 6, pp. 3031–3039, Dec. 2017.

[3] X. Zhao, S. Li, Q. Wang, M. Wang, S. Sun, and W. Hong, "Channel measurements, modeling, simulation and validation at 32 GHz in outdoor microcells for 5G radio systems," *IEEE Access*, vol. 5, pp. 1062–1072, 2017.

[4] A. Alkhateeb, Y.-H. Nam, J. Zhang, and R. W. Heath, Jr., "Massive MIMO combining with switches," *IEEE Wireless Commun. Lett.*, vol. 5, no. 3, pp. 232–235, Jun. 2016.

[5] J. Zhao, F. Gao, W. Jia, S. Zhang, S. Jin, and H. Lin, "Angle domain hybrid precoding and channel tracking for millimeter wave massive MIMO systems," *IEEE Trans. Wireless Commun.*, vol. 16, no. 10, pp. 6868–6880, Oct. 2017.

[6] M. Dai and B. Clerckx, "Multiuser millimeter wave beamforming strategies with quantized and statistical CSIT," *IEEE Trans. Wireless Commun.*, vol. 16, no. 11, pp. 7025–7038, Nov. 2017.

[7] D. H. Nguyen, L. B. Le, T. Le-Ngoc, and R. W. Heath, Jr., "Hybrid MMSE precoding and combining designs for mmWave multiuser systems," *IEEE Access*, vol. 5, pp. 19167–19181, 2017.

[8] D. Zhang, Y. Wang, and W. Xiang, "Polar decomposition based hybrid beamforming design for mmWave massive MIMO systems," in *Proc. IEEE Global Commun. Conf. (GLOBECOM)*, Dec. 2017, pp. 1–6.

[9] H. Men and M. Jin, "A low-complexity ML detection algorithm for spatial modulation systems with M PSK constellation," *IEEE Commun. Lett.*, vol. 18, no. 8, pp. 1375–1378, Aug. 2014.

[10] R. Qian, M. Sellathurai, and X. M. Fang, "Antenna selection for multi-user MIMO at millimeter-wave spectrum with lens antenna arrays," in *Proc. IEEE Int. Conf. Commun. (ICC)*, May 2017, pp. 1–5.

[11] D. Zhang, Y. Wang, X. Li, and W. Xiang, "Hybridly connected structure for hybrid beamforming in mmWave massive MIMO systems," *IEEE Trans. Commun.*, vol. 66, no. 2, pp. 662–674, Feb. 2018.

[12] L. He, J. Wang, and J. Song, "Spatial modulation for more spatial multiplexing: RF-chain-limited generalized spatial modulation aided MM-Wave MIMO with hybrid precoding," *IEEE Trans. Commun.*, vol. 66, no. 3, pp. 986–998, Mar. 2018.

[13] B. Wang, L. Dai, Z. Wang, N. Ge, and S. Zhou, "Spectrum and energy-efficient beamspace MIMO-NOMA for millimeter-wave communications using lens antenna array," *IEEE J. Sel. Areas Commun.*, vol. 35, no. 10, pp. 2370–2382, Oct. 2017.

[14] A. M. A. Abdo, X. Zhao, Z. Zhou, Y. Zhang, and O. B. Alzain, "MU-MIMO downlink sum rate analysis based on SLNR and optimum code vector design for millimeter wave communications," in *Proc. ICWMMN*, Beijing, China, 2017, p. 7.

[15] A. Alkhateeb, R. W. Heath, Jr., and G. Leus, "Achievable rates of multi-user millimeter wave systems with hybrid precoding," in *Proc. IEEE Int. Conf. Commun. Workshop (ICCW)*, Jun. 2015, pp. 1232–1237.

[16] A. Alkhateeb, G. Leus, and R. W. Heath, Jr., "Limited feedback hybrid precoding for multi-user millimeter wave systems," *IEEE Trans. Wireless Commun.*, vol. 14, no. 11, pp. 6481–6494, Nov. 2015.

[17] D. H. N. Nguyen, L. B. Le, and T. Le-Ngoc, "Hybrid MMSE precoding for mmWave multiuser MIMO systems," in *Proc. IEEE Int. Conf. Commun. (ICC)*, May 2016, pp. 1–6.

[18] Y. Chen, S. Boussakta, C. Tsimenidis, J. Chambers, and S. Jin, "Low complexity hybrid precoding in finite dimensional channel for massive MIMO systems," in *Proc. 25th Eur. Signal Process. Conf. (EUSIPCO)*, Aug./Sep. 2017, pp. 883–887.

[19] L. Zhao, D. W. K. Ng, and J. Yuan, "Multi-user precoding and channel estimation for hybrid millimeter wave systems," *IEEE J. Sel. Areas Commun.*, vol. 35, no. 7, pp. 1576–1590, Jul. 2017.

[20] T. Oh, C. Song, J. Jung, and I. Lee, "A new RF beam training method for multi-user millimeter wave systems," in *Proc. IEEE Int. Conf. Commun. (ICC)*, May 2017, pp. 1–6.

[21] J. Choi, "Beam selection in mm-wave multiuser MIMO systems using compressive sensing," *IEEE Trans. Commun.*, vol. 63, no. 8, pp. 2936–2947, Aug. 2015.

[22] Y. Zou, Q. Li, G. Yang, and X. Cheng, "Analog beamforming for millimeter-wave MIMO systems via stochastic optimization," in *Proc. 8th Int. Conf. Wireless Commun. Signal Process. (WCSP)*, Oct. 2016, pp. 1–5.

[23] J.-C. Chen, "Efficient codebook-based beamforming algorithm for millimeter-wave massive MIMO systems," *IEEE Trans. Veh. Technol.*, vol. 66, no. 9, pp. 7809–7817, Sep. 2017.

[24] (2007). *Winner II Channel Models*. [Online]. Available: http://www.cept.org/files/1050/documents/winner2%20%20final%20report.pdf
[25] G. Lee, Y. Sung, and J. Seo, "Randomly-directional beamforming in millimeter-wave multiuser MISO downlink," *IEEE Trans. Wireless Commun.*, vol. 15, no. 2, pp. 1086–1100, Feb. 2016.
[26] R. W. Heath, Jr., "Coverage and capacity analysis of mmWave cellular systems," presented at the Int. Conf. Commun. (ICC), 2013. [Online]. Available: https://www.math.ucdavis.edu/~hunter/intro_analysis_pdf/ch6.pdf
[27] J. G. Andrews, T. Bai, M. N. Kulkarni, A. Alkhateeb, A. K. Gupta, and R. W. Heath, Jr., "Modeling and analyzing millimeter wave cellular systems," *IEEE Trans. Commun.*, vol. 65, no. 1, pp. 403–430, Jan. 2017.

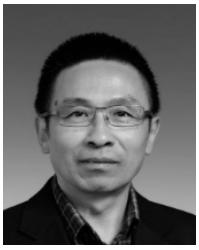

XIONGWEN ZHAO (SM'06) received the Ph.D. degree (Hons.) from the Helsinki University of Technology (TKK), Finland, in 2002. From 1992 to 1998, he was with the Laboratory of Communications System Engineering, China Research Institute of Radiowave Propagation, where he was a Director and a Senior Engineer. From 1999 to 2004, he was with the Radio Laboratory, TKK, as a Senior Researcher and a Project Manager in the areas of MIMO channel modeling and measurements at 2, 5, and 60 GHz as well as UWB. From 2004 to 2011, he was with Elektrobit Corporation, Espoo, Finland, as a Senior Specialist at EB Wireless Solutions. From 2004 to 2007, he worked in the European WINNER Project as a Senior Researcher in MIMO channel modeling for 4G radio systems. From 2006 to 2008, he also worked in the field of wireless network technologies such as WiMAX and wireless mesh networks. From 2008 to 2009, he worked in mobile satellite communications for GMR-1 3G, DVB-SH RF link budget, and antenna performance evaluations. He is currently a Professor in wireless communications with North China Electric Power University, Beijing, and chairs several projects at the National Science Foundation of China, the Key Program of the Beijing Municipal Natural Science Foundation, Beijing Municipal Science and Technology Commission, and the State Key Laboratories and Industries on Channel Measurements, Modeling, and Simulations. He is a Fellow of the Chinese Institute of Electronics. He was a recipient of the IEEE Vehicular Technology Society Neal Shepherd Memorial Best Propagation Paper Award, in 2014. He served as a TPC Member, the Session Chair, and a Keynote Speaker for numerous international and national conferences. He is a Reviewer of the IEEE transactions, journals, letters, and conferences.

ADAM MOHAMED AHMED ABDO was born in El-fashier, Sudan. He received the bachelor's and master's degrees from the School of Electronic Engineering, Sudan University of Science and Technology, in 2007 and 2014, respectively. He is currently pursuing the Ph.D. degree with North China Electric Power University. From 2014 to 2015, he was a Senior Lecturer with the Faculty of Engineering Science, Electrical and Electronic Department, University of Nyala, Sudan. His research interests include massive MIMO technology and developing new algorithms for fifth generation millimeter-wave communications.

YU ZHANG received the B.Sc. degree from North China Electric Power University, in 2016, where she is currently pursuing the Ph.D. degree in communications engineering. Her research interests include 5G networks, millimeter-wave communications, and MIMO systems.

SUIYAN GENG received the M.Sc. (Tech.) and Ph.D. degrees from the Helsinki University of Technology (TKK), Espoo, Finland, in 2003 and 2011, respectively. From 1992 to 1998, she was a Research Engineer with the China Research Institute of Radiowave Propagation, Xinxiang, China. From 2001 to 2011, she was a Research Engineer with the Radio Laboratory (Department of Radio Science and Engineering since 2008), TKK. She is currently an Associate Professor with North China Electric Power University. She was a recipient of the IEEE Vehicular Technology Society Neal Shepherd Memorial Best Propagation Paper Award, in 2014. Her research interests include millimeter-wave and ultra-wideband radio wave propagation and stochastic channel modeling for future-generation radio systems and technologies.

JIANHUA ZHANG received the Ph.D. degree in circuit and system from the Beijing University of Posts and Telecommunication (BUPT), in 2003. She is the Drafting Group Chairwoman of the ITU-R IMT-2020 channel model. She is currently a Professor with BUPT. She has published more than 100 articles in refereed journals and conferences, and holds 40 patents. Her current research interests include 5G, artificial intelligence, data mining, especially in massive MIMO and millimeter-wave channel modeling, channel emulators, and OTA test. She is a Senior Member of the IEEE. She was a recipient of the 2008 Best Paper Award of the *Journal of Communication and Network*. In 2007 and 2013, she received two national novelty awards for her contribution to the research and development of beyond 3G TDD demo system with 100 Mb/s at 20 MHz and 1 Gb/s at 100 MHz, respectively. In 2009, she received the Second Prize for science novelty from the Chinese Communication Standards Association for her contributions to ITU-R 4G (ITU-R M.2135) and 3GPP relay channel model (3GPP 36.814). From 2012 to 2014, she did 3-D channel modeling work and contributed to 3GPP 36.873, and she is also a member of 3GPP "5G channel model for bands up to 100 GHz."